Article

Chinese Science Bulletin

Environmental Chemistry

February 2011 Vol.56 No.4-5: 391–396
doi: 10.1007/s11434-010-4313-y

Temperature dependent kinetics of the gas-phase reaction of OH radicals with EMS

WANG Kun[1,2], GE MaoFa[1*] & WANG WeiGang[1]

[1]*Beijing National Laboratory for Molecular Sciences (BNLMS), State Key Laboratory for Structural Chemistry of Unstable and Stable Species, Institute of Chemistry, Chinese Academy of Sciences, Beijing 100190, China;*
[2]*Graduate School of Chinese Academy of Sciences, Beijing 100049, China*

Received August 7, 2009; accepted November 11, 2009

Using an improved smog chamber system, the temperature dependence of OH radical reaction with EMS was investigated over the temperature range of 297–346 K at 1.01×10^5 Pa pressure of air. The Arrhenius expression of the reaction was obtained for the first time. The mechanism of the reaction was also investigated.

smog chamber, temperature dependence, OH radicals, mechanism, sulfide

Citation: Wang K, Ge M F, Wang W G. Temperature dependent kinetics of the gas-phase reaction of OH radicals with EMS. Chinese Sci Bull, 2011, 56: 391–396, doi: 10.1007/s11434-010-4313-y

A large number of volatile sulfur compounds are emitted into the atmosphere by natural and anthropogenic activities. These sulfur-containing compounds, including SO_2, COS, H_2S, alkyl sulfides and alkyl thiols play an important role in both the tropospheric and stratospheric budget of atmospheric gases. It is reported that there are certain relationships between organosulfur compounds and acidity precipitation in remote areas [1]. Sulfur-containing compounds, especially dimethyl sulfide (DMS, CH_3SCH_3), are believed to be directly relevant to the formation of sulfur aerosol and cloud in marine air, and thus is potentially important in regulating cloud optical properties and climate on a global scale [2–4].

Among sulfur-containing compounds, reduced sulfur compounds including alkyl sulfide and alkyl thiol, especially DMS, have been a subject of intense scientific interest for many years. Articles on the atmospheric oxidation of various types of reduced sulfur compounds are given by Atkinson and Carter [5], Yin et al. [6], Atkinson [7,8], Tyndall and Ravishankara [9], Barnes el al. [10*]*, and Wine et al. [11]. In these articles, the kinetics, products and mechanisms of atmospheric oxidations of the major reduced sulfur compounds in the atmosphere were studied and the importance of reduced sulfur compounds (especially DMS) in the atmosphere was discussed. In 2006, Barnes et al. [12] reviewed the studies on dimethyl sulfide (DMS), dimethyl sulfoxide (DMSO) and their oxidation in the atmosphere, which emphasize the importance of sulfur-containing compounds further.

The dominant fate of reduced sulfur compounds in the atmosphere is chemical transformation, including reactions with ozone, OH radicals (under day-time conditions) and NO_3 radicals (under night-time conditions). In our previous studies, we investigated the gas phase reaction of alkyl sulfide with ozone using our smog chamber system [13–15]. The results reveal that in the atmosphere alkyl sulfides are mainly scavenged by the reaction with OH radicals and NO_3 radicals. In the present work, to test our improved smog chamber system and expand our understanding of the atmospheric fate of alkyl sulfide, we conducted relative rate measurements of ethyl methyl sulfide (EMS, $C_2H_5SCH_3$) with OH radicals over the temperature range of 297–346 K at 1.01×10^5 Pa pressure of air.

*Corresponding author (email: gemaofa@iccas.ac.cn)

1 Experimental

1.1 Apparatus

The smog chamber used here is similar to that we reported in previous publication [14]. A few improvements were made for better determination. Hence just a brief description is provided here. The reactor used is actually a 100L FEP Teflon film bag housed in a light-tight box made of iron. At the two ends of the reactor, there is an inlet and an outlet made of Teflon, respectively, facilitating the introduction of reactants and sampling. The interlayer of the box is filled with basalt fiber to maintain the temperature. The chamber is equipped with a self-made system for temperature regulation within ±0.5 K from ambient temperature to 400 K.

The reaction chamber is also equipped with a gas chromatograph with flame ionization detection (GC/FID) (GC6820, Agilent Technologies) for detection of reactants and products in the reactor. A stainless steel gas valve coupled with a 0.5-mL steel loop was fixed on the GC for gas sampling. During the experiments, to avoid the great absorption of EMS on the steel tube of the valve, the steel tube was changed to Teflon tube, and the valve was heated to 430 K. The gas samples were collected from the chamber by a windtight syringe and injected into the GC coupled with a 15m DB-1 capillary column (0.53 mm i.d., 1.5 μm phase).

1.2 Procedure

The kinetic experiments for determining rate coefficients for the reaction of OH radicals with EMS were performed at a total pressure of 1.01×10^5 Pa synthetic air and six different temperatures (297, 310.5, 316, 326, 336 and 346 K). Cyclohexane, whose rate coefficient for the reaction with OH radicals is well established, was used as the reference compound in this investigation. The photolysis of hydrogen peroxide (H_2O_2) was used as the OH radical source:

$$H_2O_2 + h\nu \xrightarrow{254\ \text{nm}} 2\text{OH}\bullet$$

The starting concentrations (calculated at the working temperature) of EMS and the reference organic compounds were typically in the range of about (0.7–2.6) $\times10^{15}$ molecule cm^{-3} and that of H_2O_2 was approximately (1.48–2.6) $\times10^{15}$ molecule cm^{-3}. It was observed that for both gaseous and liquid organics, these calculated concentrations agreed within ±10% with the concentrations quantitatively measured by gas chromatography. In a typical experiment, the concentration of EMS and the reference compound in the chamber was measured every 5–8 min, and the experiment lasted for about 2 h.

The rate coefficient for the reaction of EMS with OH radicals was determined using a relative rate method in which the relative disappearance rates of EMS and the reference compound are monitored synchronously in the presence of OH radicals:

$$\text{EMS}+\text{OH}\bullet \xrightarrow{k_s} \text{Products} \quad (1)$$

$$\text{Reference}+\text{OH}\bullet \xrightarrow{k_r} \text{Products} \quad (2)$$

Given that EMS and the reference are removed solely by the reaction with OH radicals, eq. (I) can be obtained in the following form

$$\ln\left(\frac{C_{\text{EMS},0}}{C_{\text{EMS},t}}\right)=\frac{k_s}{k_r}\ln\left(\frac{C_{\text{ref},0}}{C_{\text{ref},t}}\right), \quad (\text{I})$$

where $C_{\text{EMS},0}$ and $C_{\text{ref},0}$ are the concentrations of EMS and the reference compound, respectively, at the beginning of the experiment; $C_{\text{EMS},t}$ and $C_{\text{ref},t}$ are the corresponding concentrations at time t; k_s and k_r are the rate coefficients for the reactions of OH radicals with EMS and the reference compound, respectively.

The photo-stability of EMS and cyclohexane was established by irradiation of EMS-cyclohexane-air mixtures in the absence of OH radical precursors for a time period as long as that employed in the kinetic experiments, after switching on the lamps. Cyclohexane was not photolysed and its wall losses were within the variation coefficient for duplicate injections. For EMS, wall losses represented by reaction (3) accounted for approximately 7% of its measured decay under irradiation conditions at room temperature and the rate coefficient for wall losses (k_{wall}) decreased gradually to zero at the highest temperature employed in the experiments.

$$\text{EMS}+\text{M(wall)} \xrightarrow{k_{\text{wall}}} \text{Products} \quad (3)$$

Thus, incorporating the first-order wall loss process of EMS into eq. (I) leads to eq. (II),

$$\ln\left(\frac{C_{\text{EMS},0}}{C_{\text{EMS},t}}\right)-k_{\text{wall}}\times t=\frac{k_s}{k_r}\ln\left(\frac{C_{\text{ref},0}}{C_{\text{ref},t}}\right). \quad (\text{II})$$

In every experiment, to avoid the error caused by the slight difference in EMS wall losses, the wall decay of EMS was measured at the beginning of every experiment by recording 8–10 GC spectra prior to irradiation. According to eq. (II), a plot of $\ln(C_{\text{EMS},0}/C_{\text{EMS},t}) - k_{\text{wall}}\times t$ against $\ln(C_{\text{ref},0}/C_{\text{ref},0})/k_r$ gives straight lines directly yielding k_s as the slope.

1.3 Reagents

Ethyl methyl sulfide was supplied by Aldrich with a stated purity of 99%. Cyclohexane with purity of 99% was purchased from Alfa Aesar. Ethanol and methanol were supplied by Beijing Beihua Fine Chemcials Co., Ltd with the purity of 99% and 99.5%, respectively. All liquid organics were thoroughly degassed through a series of freeze-pump-thaw cycles at 77 K to remove the impurities. The following

gases were supplied by Beijing AP Gas Industry Co., Ltd: nitrogen (99.999%) and oxygen (99.999%). Synthetic air was the mixture of N_2 and O_2 with a volume ratio of 4:1. H_2O_2 (30 wt%) from Beijing Beihua Fine Chemcials Co., Ltd. was condensed from 30% to about 80% by vacuum distillation.

2 Results and discussion

2.1 Kinetics of OH radicals with ethanol

As a testing experiment, the OH rate constant for ethanol was obtained using the apparatus described above. The experiments were conducted at 298 K under 1.01×10^5 Pa and N_2 was used as the buffer gas. The use of cyclohexane ($k_{\text{cyclohexane+OH}}=6.7\times10^{-12}$ cm^3 molecule^{-1} s^{-1}) [16] and methanol ($k_{\text{methanol+OH}}=9.28\times10^{-13}$ cm^3 molecule^{-1} s^{-1}) [17] as reference compounds resulted in the OH + ethanol rate constant of (3.23±0.29) and $(3.49\pm0.47)\times10^{-12}$ cm^3 molecule^{-1} s^{-1}, respectively. For both reference compounds, the determination was conducted in three different ethanol concentration conditions. The combined plots, which are a modified version of eq. (I) (here in eq. (I), [EMS] is changed to [ethanol]), are shown in Figure 1. For each reference compound, only one plot derived from a typical experiment is listed here. A linear least-squares analysis of the plots gives the rate constants for the OH + ethanol reaction. Incorporating the uncertainties associated with the reference rate constants used to derive the OH + ethanol rate constant yields a final value for $k_{\text{ethanol+OH}}$ of $(3.26\pm0.35)\times10^{-12}$ cm^3 molecule^{-1} s^{-1}. The results obtained in this work together with those found in the literatures for ethanol + OH radicals are summarized in Table 1.

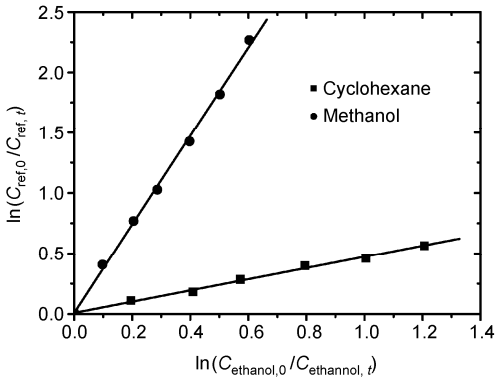

Figure 1 Plots of the kinetics data for ethanol + OH reaction according to eq. (I) with cyclohexane and methanol as the reference compounds.

Table 1 Summary of the rate constants for the reaction of ethanol with OH radicals obtained in previous studies

T_{range} (K)	k_{298} (10^{-12} cm^3 molecule^{-1} s^{-1})	Technique	Reference
240–440	3.31	FP-RF	18
205–450	3.40	review	19
227–360	3.23	LP-LIF	20
210–351	3.26	FP-LIF	21
298	3.04±0.25	FP-UV	22
295	3.4±0.25[a)]	GC	23

a) The rate constant in Reference 23 was measured at 295 K.

As seen in Table 1, our result agrees well with the previous values obtained in absolute methods [18–22] and the result obtained by Wu et al. [23] by similar technique. We could believe that our smog chamber system is suitable for the simulation of gas phase reactions of OH radicals with VOC.

2.2 Kinetics of OH reaction with EMS

(1) Influences of adsorption and particles. Using the apparatus proved suitable above, experiments were conducted to investigate OH + EMS rate constant at 298 K and 1.01×10^5 Pa pressure. Initially, experiments performed under different concentrations of EMS, cyclohexane and H_2O_2 (80 wt%) were repeated for more than 20 times, and repeated puzzling curving plots derived from eq. (II) were obtained. The concentration conditions of a part of these experiments are listed in Table 2 and the combined plots are shown in Figure 2.

A careful comparison was made to analyse the reasons for the puzzling curving plots. Comparison between the results of experiments 1–3 shows that H_2O_2 concentration influences the extent to which the curving plots differ from the normal linear plots. However, if the conversion ratio of experiments 1–3 was considered, the agreement between these experiments at the same conversion ratio is good.

As shown in Figure 2, the initial part of each plot exhibits

Table 2 Concentration conditions of a part of the initial experiments

Experiment No.	EMS (10^{15} molecule cm^{-3})	Cyclohexane (10^{15} molecule cm^{-3})	H_2O_2 (10^{15} molecule cm^{-3})
1	1.22	0.83	1.48
2	1.22	0.83	1.84
3	1.22	0.83	2.6
4	0.70	0.83	1.48
5	1.84	0.83	2.6
6	2.60	0.83	2.6

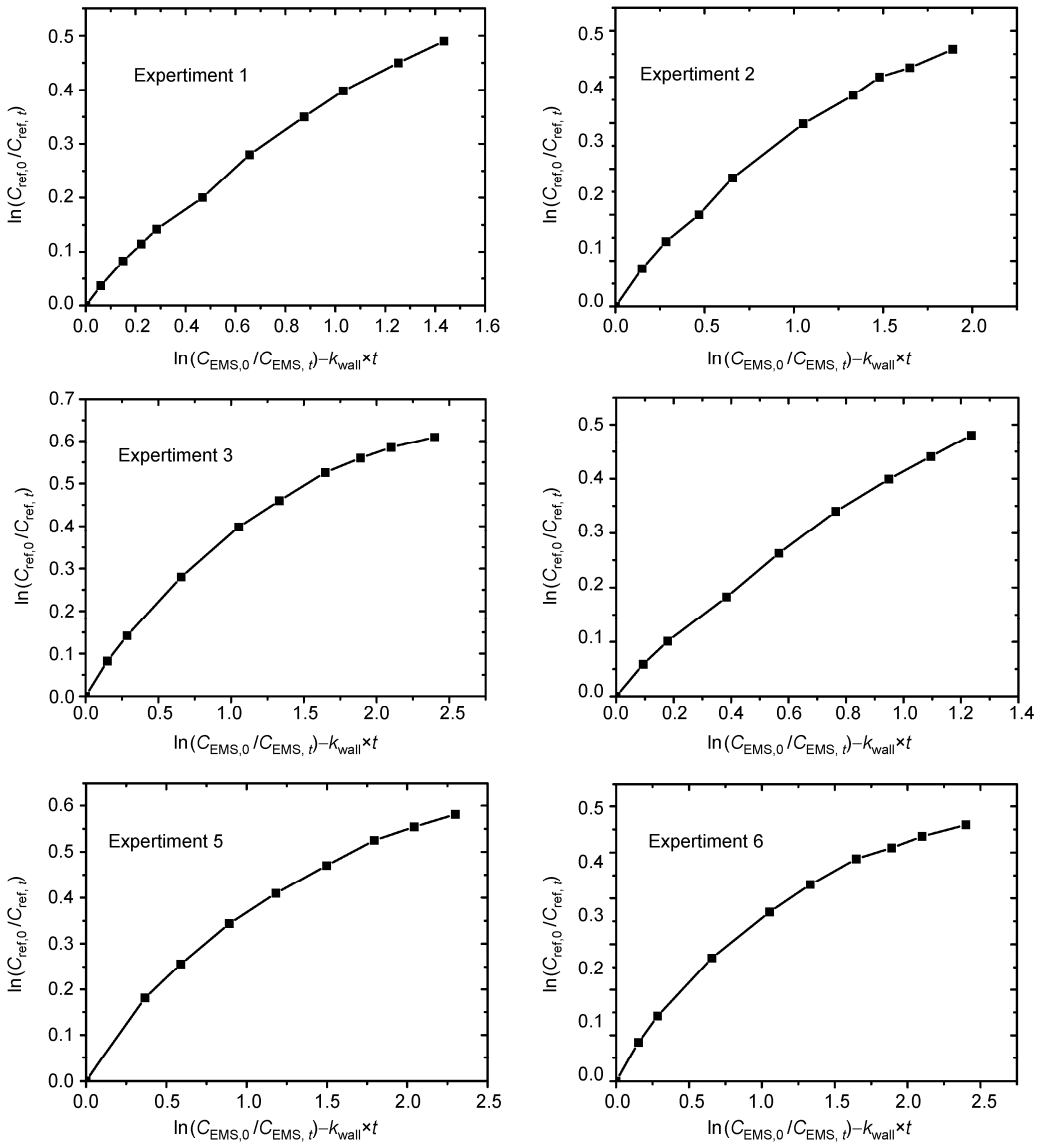

Figure 2 Plots of the kinetics data for experiments 1–6.

good linearity and the agreement between these initial parts is very good. For each experiment, the plot derived always exhibits good linearity in the initial part and becomes more and more curving with the proceeding of the reaction. Further analysis reveals that if conversion ratio of the experiments was fixed, the higher the EMS concentration is, the larger the plots will differ from normal linear plot. It has been reported that aerosols have catalytic effects on the reaction kinetics of the VOCs [24–26]. In our experiments, because of the relatively high EMS concentration and large conversion rate, we could believe the accumulation of a nice bit of small particles in the reactor. Thus, the catalytic effect of particulate matter on the oxidation rate of EMS in the presence of OH radicals may lead to the puzzling error of the plots.

To minimize the catalytic effect of particles, the conversion ratio was controlled to less than 30%. At the same time, the steps mentioned above to control the adsorption were also taken into account. Experiments under these conditions were conducted at 297 K and 1.01×10^5 Pa, and the corresponding plot for a typical experiment is listed in Figure 3. The good linearity of the plot in Figure 3 proves the necessity and validity of the steps we adopted to solve the puzzling problem of the curving plots.

(2) Temperature dependence of OH radical reaction with EMS. The rate constants for the OH radical reaction with EMS were determined under the improved experiment conditions over the temperature range of 297–346 K. The results are listed in Table 3. The data given in Table 3 are plotted in Arrhenius form in Figure 4. Unweighted linear least-squares analysis of these data leads to the following Arrhenius expressions,

$$k_{\mathrm{EMS}} = 7.25\times10^{-11}(\mathrm{cm^3\ s^{-1}\ molecule^{-1}})\mathrm{e}^{-(3.9\pm0.37)(\mathrm{kJ/mol})/RT}.$$

At room temperature (297 K), the rate constants we obtained are in good agreement with that reported by Wang

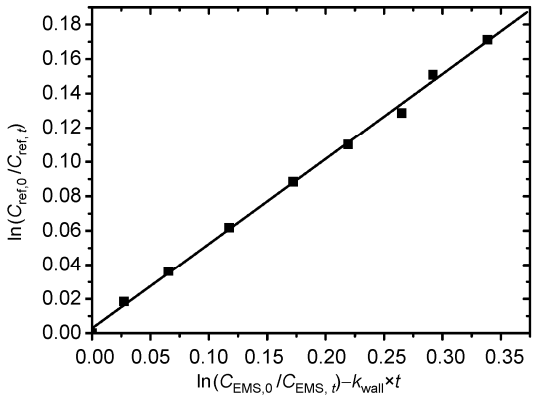

Figure 3 A typical EMS relative rate plot with cyclohexane as reference compounds under improved experiment conditions. $C_{EMS,0}$=0.61×10^{15} molecule cm^{-3}, $C_{ref,0}$=0.83×10^{15} molecule cm^{-3}.

Table 3 Rate coefficient ratio k_r/k_s and rate coefficient k_s for the gas phase reaction of OH radicals with EMS at different temperatures

T(K)	$C_{EMS,0}$ (10^{15}molecul cm^{-3})	$k'=k_r/k_s$	k_s (10^{-11}cm^3 molecule^{-1} s^{-1})
297	1.22	0.4608	1.495±0.29
	1.84	0.4575	
	2.60	0.4789	
310.5	1.22	0.4607	1.59±0.47
	1.84	0.4769	
	2.60	0.4589	
316	0.70	0.4531	1.65±0.33
	0.61	0.4659	
	1.30	0.4432	
326	1.22	0.4509	1.72±0.38
	1.84	0.4621	
	2.60	0.4473	
336	0.70	0.4520	1.78±0.22
	1.22	0.4475	
	2.60	0.4671	
346	0.68	0.4461	1.87±0.39
	1.22	0.4514	
	1.84	0.4340	

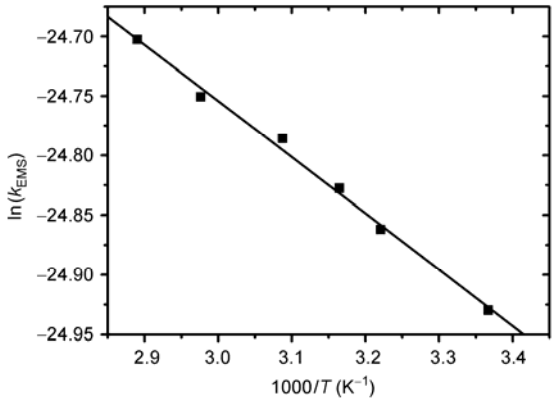

Figure 4 Arrhenius plot of the rate coefficients determined for EMS+OH over the temperature range of 297 to 346 K.

et al. [27] under similar conditions. The result of the absolute measurement reported by Hynes et al. [28] is about (8.31±0.12)×10^{-12} cm^3 molecule^{-1} s^{-1}, but their experiments were conducted at 299K and 5.31×10^3 Pa argon buffer gas. No other literature data are available.

The reaction of OH radicals with EMS is thought to proceed via both direct H atom abstraction (reaction (4)) in the absence of O_2 and reversible $CH_3S(OH)CH_2CH_3$ adduct formation (reaction (5)) in the presence of O_2:

$$OHg+CH_3SCH_2CH_3 \rightarrow CH_3S\dot{C}HCH_3+H_2O \quad (4a)$$

$$\rightarrow \dot{C}H_2SCH_2CH_3+H_2O \quad (4b)$$

$$\rightarrow CH_3SCH_2\dot{C}H_2+H_2O \quad (4c)$$

$$OHg+CH_3SCH_2CH_3 \rightarrow CH_3\dot{S}(OH)CH_2CH_3 \quad (5a)$$

$$CH_3\dot{S}(OH)CH_2CH_3+O_2 \rightarrow \text{Products} \quad (5b)$$

To the best of our knowledge, the activation energy of OH reaction with DMS is still not well characterized. Wallington et al. [29] reported a negative Arrhenius activation energy, while the studies of Wine et al. [11], Hynes et al. [28], Hsu et al. [30], and Abbatt et al. [31] report a positive Arrhenius activation energy. The latest IUPAC data evaluation recommends a positive Arrhenius activation energy. For OH radical reactions with both DMS and EMS, the observation of a positive activation energy can be taken as an indication of the dominance of the hydrogen abstraction reaction in the systems used to study the reaction, while measurement of a negative Arrhenius activation energy can be taken as an indication that the association reaction of adduct formation probably also contributes to the rate coefficient measurement under the conditions employed.

In this work, we observed a positive activation energy (3.9±0.37) kJ for OH radical reaction with EMS in the presence of O_2, which indicates the dominance of the hydrogen abstraction reaction under our experimental conditions. Although the association reaction of adduct formation should not be excluded since the air was used as the buffer gas in our system, the relatively high value of the positive activation energy seems to imply that the adduct formation reaction contributes very little to the total reaction. At temperatures below 270 K, the results of Albu et al. [32] and Williams et al. [33] show that the rate constants for OH reaction with DMS in the presence of O_2 increase with the decrease of the temperature and the contribution of adduct formation reaction becomes more and more important with the decrease of the temperature. These results are generally in fair agreement with our results.

3 Atmospheric implication

In this work, an improved smog chamber system was tested and used to investigate the temperature dependence of the gas-phase reaction of the OH radicals with EMS. At 298 K, the constant of OH radicals with ethanol was determined and the results proved our smog chamber is suitable for the

simulation of gas phase reactions of OH radicals with VOC.

Using the tested smog chamber system, the OH radical reaction with EMS was investigated over the temperature range of 297–346 K under 1.01×10^5 Pa pressure and the obtained Arrhenius expression is $k_{EMS}=7.25\times10^{-11}$ ($cm^3\ s^{-1}$ $molecule^{-1}$)$e^{-(3.9\pm0.37)(kJ/mol)/RT}$. Investigation of the mechanism of the reaction reveals that at temperatures over 298 K, the H abstraction reaction is the major channel of the reaction.

During the initial experiments, it is found that when the conversion ratio of the EMS+ OH reaction is large enough, the rate constant increases with the proceeding of the reaction. It seems that the sulfate particles formed during the reaction has a catalytic effect on the reaction. In China, because of the wide use of coal as the energy source, the average content of sulfate aerosol is much higher than that in the Northern Hemisphere [34]. Reduced sulfur compounds and a significant fraction of the total mass of semi-volatile compounds may be absorbed on these particles and the potential catalytic effect of the particles may influence the atmospheric oxidation of these compounds.

This work was supported by the Knowledge Innovation Program of the Chinese Academy of Sciences (*KJCX2-YW-N24, KZCX2-YW-205*) *and the National Natural Science Foundation of China* (*40830101, 40925016*).

1 Galloway J N, Likens G E, Keene W C, et al. The composition of precipitation in remote areas of the world. J Geophys Res, 1982, 87: 8771–8786
2 Andrea M O, Raemdonck H. Dimethylsulfide in the surface ocean and the marine atmosphere: A global view. Science, 1983, 221: 744–747
3 Harvey G R, Lang R F. Dimethylsulfoxide and dimethylsulfone in the marine atmosphere. Geophys Res Lett, 1986, 13: 48–51
4 Chalson R J, Lovelock J E, Andreae M O, et al. Oceanic phytoplankton, atmospheric sulphur, cloud albedo and climate. Nature, 1987, 326: 655–661
5 Atkinson R, Carter W P L. Kinetics and mechanisms of the gas-phase reactions of ozone with organic compounds under atmospheric conditions. Chem Rev, 1984, 84: 437–470
6 Yin F D, Grosjean D, Seinfeld J H. Analysis of atmospheric photooxidation mechanisms for organosulfur compounds. J Geophys Res, 1986, 91: 14417–14438
7 Atkinson R. Kinetics and mechanisms of the gas-phase reactions of thehydroyl radical with organic compounds. J Phys Chem Ref Data, 1989, Monograph 1: 1–246
8 Atkinson R. Gas-phase tropospheric chemistry of organic compounds. J Phys Chem Ref Data, 1994, Monograph 2: 1–216
9 Tyndall G S , Ravishankara A R. Kinetics of the reaction of the methylthiol radical with ozone at 298 K. J Phys Chem, 1989, 93: 4707–4710
10 Barnes I, Bastian V, Berker K H, et al. Oxidation of sulphur compounds in the atmosphere: I. Rate constants of OH radical reactions with sulphur dioxide, hydrogen sulphide, aliphatic thiols and thiophenol. J Atmos Chem, 1986, 4: 445–466
11 Wine P H, Kreutter N M, Gump C A, et al. Kinetics of OH reactions with atmospheric sulfur compounds H_2S, CH_3SH, CH_3SCH_3 and CH_3SSCH_3. J Phys Chem, 1981, 85: 2660–2665
12 Barnes I, Hjorth J, Mihalopoulos N. Dimethyl sulfide and dimethyl sulfoxide and their oxidation in the atmosphere. Chem Rev, 2006, 106: 940–975
13 Du L, Xu Y F, Ge M F, et al. Rate constant of the gas phase reaction of dimethyl sulfide (CH_3SCH_3) with ozone. Chem Phys Lett, 2007, 436: 36–40
14 Du L, Xu Y F, Ge M F, et al. Rate constant for the reaction of ozone with diethyl sulfide. Atmos Environ, 2007, 41: 7434–7439
15 Wang K, Du L, Ge M F. Rate constants for the reaction of ozne with n-butyl, s-butyl and t-butyl methyl sulfides. Chinese Sci Bull, 2008, 53: 3620–3625
16 Atkinson R. Kinetics of the gas-phase reactions of OH radicals with alkanes and cycloalkanes. Atmos Chem Phys, 2003, 3: 2233–2307
17 Atkinson R, Baulch D L, Cox R A, et al. Evaluated kinetic, photochemical and heterogeneous data for atmospheric chemistry: Supplement V, IUPAC subcommittee on gas kinetic data evaluation for atmospheric chemistry. J Phys Chem Ref Data, 1997, 26: 521–1011
18 Wallington T J, Kurylo M J. The gas phase reactions of hydroxyl radicals with a series of aliphatic alcohols over the temperature range 240–440 K. Int J Chem Kinet, 1987, 19: 1015–1023
19 Atkinson R, Baulch D L, Cox R A, et al. Evaluated kinetic and photochemical data for atmospheric chemistry: Supplement III. J Phys Chem Ref Data, 1989, 18: 3881–1097
20 Jimenez E, Gilles M K, Ravishankara A R. Kinetics of the reactions of the hydroxyl radical with CH_3OH and C_2H_5OH between 235–360 K. J Photochem Photobio A Chem, 2003, 157: 237–245
21 Dillon T J, Holscher D, Sivakumaran V, et al. Kinetics of the reactions of OH with methanol (210–351 K) and with ethanol (216–368 K). Phys Chem Chem Phys, 2005, 7: 349–355
22 Nelson L, Rattigan O, Neavyn R, et al. Absolute and relative rate constants for the reactions of hydroxyl radicals and chlorine atoms with a series of aliphatic alcohols and ethers at 298 K. Int J Chem Kinet, 1990, 22: 1111–1122
23 Wu H, Mu Y J, Zhang X S, et al. Relative rate constants for the reactions of hydroxyl radicals and chlorine atoms with a series of aliphatic alcohols. Int J Chem Kinet, 2003, 35: 81–87
24 Guillard C, Delprat H, Hoang-Van C, et al. Laboratory study of the rates and products of the photo transformations of naphthalene adsorbed on samples of titanium dioxide, ferric oxide, muscovite, and fly ash. J Atmos Chem, 1993, 16: 47–59
25 Ammann M, Kalberer M, Jost D T, et al. Heterogeneous production of nitrous acid on soot in polluted air masses. Nature, 1998, 395: 157–160
26 Behnke W, Hollander W, Koch W, et al. A smog chamber for studies of the photochemical degradation of chemicals in the presence of aerosols. Atmos Environ, 1988, 22: 1113–1120
27 Wang H T, Zhang Y J, Mu Y J. Rate Constants for reactions of •OH with several reduced sulfur compounds determined by relative rate constant method. Acta Phys Chim Sin, 2008, 24: 945–950
28 Hynes A J, Wine P H, Semmes D H. Kinetics and mechanism of OH reactions with organic sulfides. J Phys Chem, 1986, 90: 4148–4156
29 Wallington T J, Atkinson R, Tuazon E C et al. The reaction of OH radicals with dimethyl sulfide. Int J Chem Kinet, 1986, 18: 837–846
30 Hsu Y C, Chen D S, Lee Y P. Rate constants for the reaction of OH radicals with dimethyl sulfide. Int J Chem Kinet, 1987, 19: 1073–1082
31 Abbatt J P D, Fenter F F, Anderson J G. High-pressure discharge flow kinetics study of OH + CH_3SCH_3, CH_3SSCH_3 from 297 to 368 K. J Phys Chem, 1992, 96: 1780–1785
32 Albu M, Barnes I, Becker K H, et al. Rate coefficients for the gas-phase reaction of OH radicals with dimethyl sulfide: Temperature and O_2 partial pressure dependence. Phys Chem Chem Phys, 2006, 8: 728–736
33 Williams M B, Jost P C, Bauer D, et al. Kinetic and mechanistic studies of the OH- initiated oxidation of dimethylsulfide at low temperature—A reevaluation of the rate coefficient and branching ratio. Chem Phys Lett, 2001, 344: 61–67
34 Qian Y, Wang H Q, Fu H B, et al. Seasonal and spatial variation of radiative effects of anthropogenic sulfate aerosol. Adv Atmos Sci, 1998, 15: 380–392